Long-wavelength acoustic-mode-enhanced electron emission from Se and Te donors in silicon

O. A. Korotchenkov* and H. G. Grimmeiss
Department of Solid State Physics, University of Lund, Box 118, S-221 00 Lund, Sweden
(Received 20 June 1995)

An enhancement of the thermal emission rates from Se and Te double donors in silicon was observed by applying external vibrational excitation in the MHz frequency range. The excitation was performed either by resonant sample vibrations at frequencies of the lowest eigenmodes or by Lamb waves in a plate. Emission rates were measured by using both deep-level transient spectroscopy and single-shot capacitance techniques. Possible explanations for the observed enhancement of the emission rates are either thermal disturbances due to thermoelastic losses of mechanical energy or nonlinear effects in conjunction with oscillating stresses in solids. Our data are inconsistent with possible thermal disturbances. A tentative model is therefore proposed, suggesting that changes in the equilibrium position of impurity atoms exhibiting low-frequency oscillations yield enhanced emission rates. These changes depend upon the local surrounding of the impurity atoms and "hardness" of the interatomic interaction rather than the strength. Vibrational perturbations as discussed in this paper may be an effective tool to obtain new information on defects in solids.

I. INTRODUCTION

A better understanding of the physical nature of electronic emission and capture processes is of considerable importance for a comprehensive characterization of defects in semiconductors. Emission and capture processes are also of fundamental importance for many applications, since they determine carrier lifetimes and, hence, are critical for device performances. This is particularly true for silicon, since most devices are fabricated in silicon. However, in spite of many and very comprehensive studies, it is fair to say that our knowledge concerning the dynamical behavior of different impurities in silicon is still limited.

In general, the dynamical behavior of defects has considerable influence on their charge state, defect symmetry, and/or lattice relaxation, and these parameters are therefore often studied by investigating the dynamical properties under external perturbation. Such studies have been performed on many defects, and the chalcogen-related centers in silicon are often considered as typical examples since they are particularly well suited for studies of different field-influenced emission processes.[1] The microscopic structure of defects is, for example, often studied by using uniaxial stress, since stress changes the local crystal field. In certain cases it is, however, difficult to obtain sufficient information from such perturbation techniques. In this paper it is therefore suggested to employ external perturbation by using alternating deformations at ultrasonic frequencies in order to study thermally activated electronic processes in semiconductors. Whereas high-intensity ultrasonic waves have been used during the last 10–15 years to characterize defects originating from the motion of dislocations in semiconductors,[2] surprisingly little attention has been paid to study point defects by ultrasonic vibrations. It is nevertheless interesting to note that changes in recombination properties of charge carriers due to ultrasonic waves have been observed recently.[3]

This paper presents results which have been obtained by studying deep point defects under external perturbation by using oscillating deformations in the MHz frequency range. The amplitude of the applied deformation was too small for describing the results within the framework of dislocation dynamics. The purpose of the study was to obtain information on the electronic properties of deep impurity centers not by studying the absorption of acoustic waves, as in previous studies of internal frictions,[4] but by investigating the change of thermal ionization processes due to mechanical vibrations. The thermal emission rate of a point defect is usually expressed in terms of enthalpy and entropy changes, and therefore depends upon the dynamical behavior of the defect. Since the change in defect dynamics due to external vibrational perturbation is defect specific, it is reasonable to believe that such measurements may provide interesting information about the electronic properties of point defects.

II. EXPERIMENTAL DETAILS

The samples used in this paper were selenium- and tellurium-doped p^+-n diodes. The crystals were aligned along the principal axes of the silicon cell such that the shortest dimensions corresponded to the ⟨100⟩ axes in all samples and the p-n junctions were parallel to the (100) surfaces. The procedure for the preparation of p-n junctions was similar to the one previously published.[5,6] Both resonant sample vibration and acoustic wave propagation regimes have been used. The data presented below were obtained on three samples with dimensions $0.53\times1.65\times2.10$ mm^3 (Se doped), $0.53\times2.2\times13.6$ mm^3 (Se doped), and $0.41\times2.20\times2.40$ mm^3 (Te doped). The two smaller samples were used for the resonant vibration technique, whereas the wave propagation regime was applied in the longest sample.

In the resonant vibration technique, the samples were placed between two zirconate-titanate piezoceramic transducers, as shown in Fig. 1(a). One of the transducers was used as a vibration generator whereas the other transducer was used as a detector of the resonant response. The transducers were mounted on the sample by using epoxy glue both with and without hardening components. In order to identify the sample resonances, two pairs of different piezotransducers with thickness resonant frequencies of about 3 and 8 MHz, respectively, were applied. A careful check was performed to ensure that the transducers were linear in the applied voltage range. All results discussed in this paper were obtained with transducers which had thickness resonant frequencies above 2.9 MHz. None of the transducers showed vibrational modes in the frequency range 0.8–2.8 MHz.

A calibration of the stresses was performed by infrared-absorption measurements with a Bomem DA3.02 Fourier-transform spectrometer. A Se-doped silicon sample similar to those previously used in uniaxial-stress measurements[7] was mounted into the resonant cell shown in Fig. 1(a). From the observed broadening of the Se^0 absorption lines, the maximum amplitude of stress in the vicinity of the impurity atom was estimated to be $\theta_0 \sim 5\times10^5$ N/m^2. The applied stress was therefore continuously variable between 0 and θ_0, corresponding to rf voltage amplitudes A_{in} between 0 and 8 V at frequencies of the lowest longitudinal eigenmodes.

Acoustic wave propagation was achieved by placing similar piezotransducers on the sample surface, as shown in Fig. 1(b). Again, one of them served as the driver, whereas the other served as the receiver of the propagated waves. By applying a voltage A_{in} to the transducer, an antisymmetric a_0 mode of Lamb waves[8] was generated in the chosen frequency range.

Emission rates were studied by using deep-level transient spectroscopy (DLTS) and single-shot capacitance measurements. Either a DLS-83D spectrometer or a boxcar-based technique was employed. The measurements were performed at reverse biases of 1.5 and 2.0 V and in the temperature region between 77 and 350 K with the samples mounted in a temperature variable Leybold continuous-flow cryostat. The sample temperature was measured with a Cu-Constantan thermocouple directly attached to the sample. Repeated measurements showed that the DLTS peak temperature was reproducible to better than 0.1 K when measured by the DLTS spectrometer. To ensure temperature uniformity, the temperature change was slow, i.e., about 0.03 K/s.

It was also verified that our experimental systems were not susceptible to electronic pickups or ground loop effects. Measurements taken in different samples at temperatures with no DLTS signal displayed no system response when the exciting rf signal was applied. In principle, no changes were observed when an epoxy resin bar, 2 mm long and 7 mm in diameter, with metallized and grounded surfaces was placed between the sample and transducer. In this case, the sample was coupled through its largest side to the bar, acting as a wave guide.

The time sequences of voltage pulses and ultrasonic tonebursts used in our boxcar-based DLTS measurements are shown in Fig. 2. After short-circuiting the diode a time τ_p (filling pulse), a reverse bias U_b was applied during the time $t_0-\tau_p$, causing a capacitance transient $C(t)$. The capacitance transient $C(t)$ was measured at two

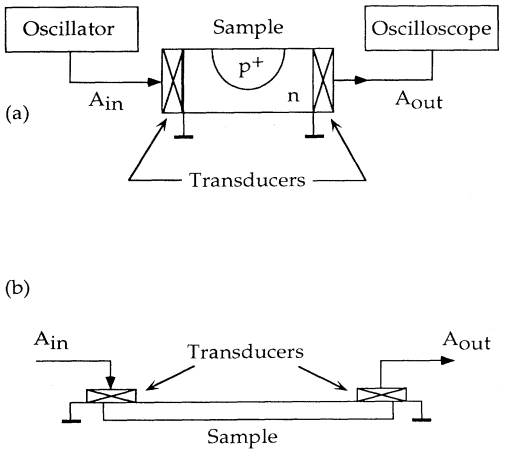

FIG. 1. Schematic diagram of the experimental cells which have been used to excite samples by resonant vibrations (a) and Lamb waves (b).

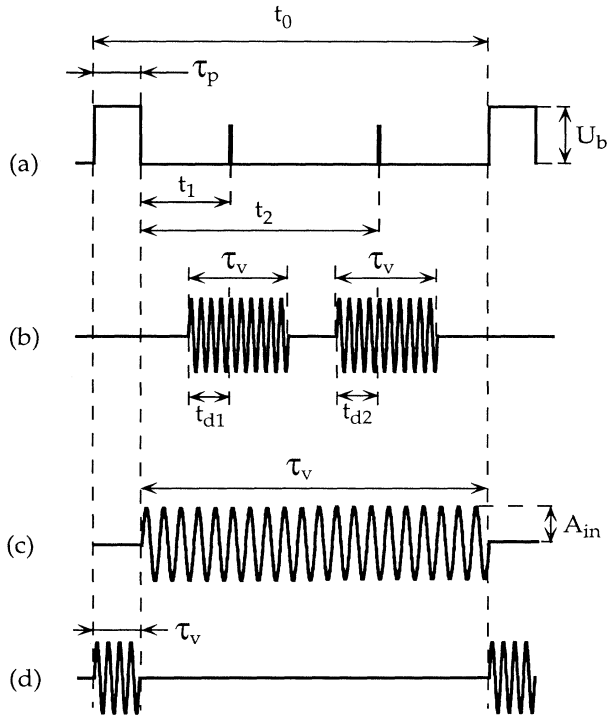

FIG. 2. Time sequence of voltage pulses in the boxcar-based technique (a) and of ultrasonic tonebursts [(b), (c), and (d)] (see text for details).

different times t_1 and t_2 [Fig. 2(a)], and the difference of these two signals was monitored in the boxcar. The emission rate at the DLTS peak temperature is then given by[9]

$$e_n^t = \ln(t_2/t_1)/(t_2-t_1) \ . \quad (1)$$

The time dependence of the change in e_n^t caused by resonant vibrations, was measured by using a gated rf signal. In this case, the oscillator in Fig. 1(a) was controlled by a pulse generator which was synchronized with the standard boxcar technique, implying that the transducers generated ultrasonic tonebursts. By changing the length and time delay of the gating pulse, the duration τ_v of the resonant vibrations was changed and shifted along the time scale. By applying two separated tonebursts during the boxcar-determined period t_0 [Fig. 2(b)], the DLTS peak position was studied as a function of the time delay $t_d = t_{d1} = t_{d2}$. By changing the width τ_v and the delay of the toneburst [Figs. 2(c) and 2(d)], we were able to separate the external excitation and the thermal emission.

III. RESULTS AND ANALYSIS

The samples employed in this study exhibited all energy levels previously observed in Se- and Te-doped silicon.[5,10,11] The DLTS spectra showed two dominant peaks due to the charged (Se^+, Te^+) and neutral (Se^0, Te^0) version of the double donors. As an example, Fig. 3 presents the change of the DLTS signal in the case of the Se^0 center due to resonant vibrations, i.e., for a rf corresponding to the sample's natural frequency for longitudinal oscillations. Applying oscillating stress, either as resonant vibrations or acoustic waves, produced similar changes of the DLTS signal in all samples.

The observed changes can be summarized as follows: (i) With increasing amplitude of vibrations, the DLTS peaks shifted to lower temperatures; i.e., an enhanced thermal emission rate was observed. A similar increase of the thermal emission was observed in single-shot capacitance measurements. Capacitance transients obtained for Se^0 and Se^+ centers at different amplitudes of external perturbation are shown in Fig. 4. (ii) The amount of the DLTS peak shift depended on the frequency of the applied oscillations and the specific center. A typical frequency dependence is shown in Fig. 5 for the Se^0 center. A simplified calculation suggests that the high-frequency peaks A and B are due to the two fundamental longitudinal eigenmodes corresponding to the length and width of the sample, and that peak C is due to transverse oscillations. Resonant responses in the same frequency range were also detected in the output signal A_{out} [see Fig. 1(a)]. If the vibrations were reoriented 90° with respect to the previous orientation, peak A became stronger and peak B became smaller, whereas a peak close to 1.8 MHz appeared due to transverse vibrations. (iii) No splittings of the DLTS peaks were observed, only small changes of their widths. The full width at half maximum of the peak in Fig. 3, for example, changed from 29.5 K (spectrum 1) to 32.4 K (spectrum 2), accompanied by a corresponding decrease in the DLTS peak height.

Thermal excitation of electrons from deep donor centers can be considered within the adiabatic approximation. Figure 6 shows the energy configuration diagram of such a center. The upper and lower solid curves

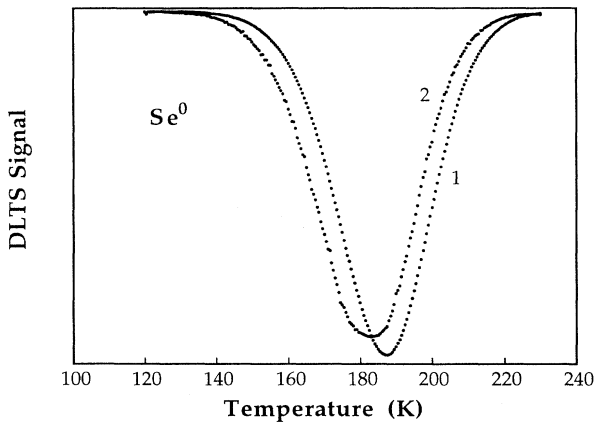

FIG. 3. DLTS scans of the Se^0 center in silicon without vibrational excitation (1) and with $A_{in} = 8$ V (2). The frequency of vibrations was 2.00 MHz. The rate window and filling pulse width were 6282 s^{-1} and 20 μs, respectively.

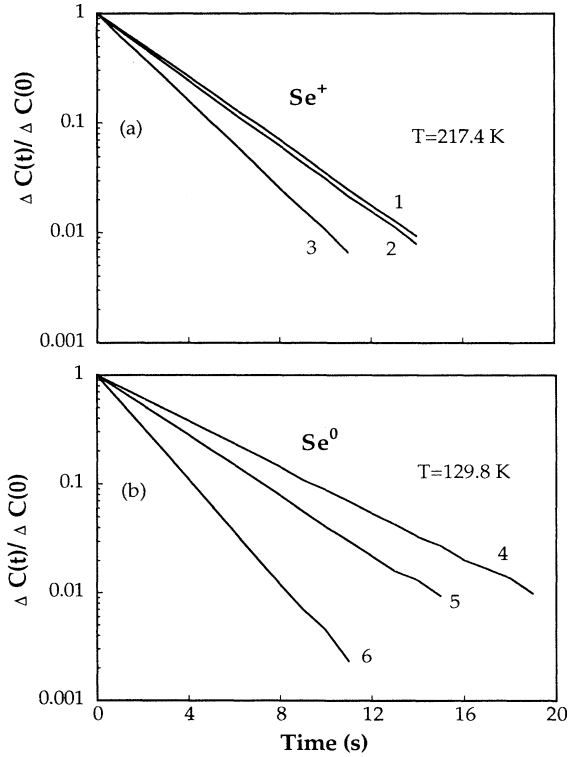

FIG. 4. Normalized capacitance transients for charged (a) and neutral (b) selenium donors measured without vibrational excitation (1,4), with $A_{in} = 4$ V (2,5) and with $A_{in} = 8$ V (3,6). The frequency of vibrations was 2.00 MHz.

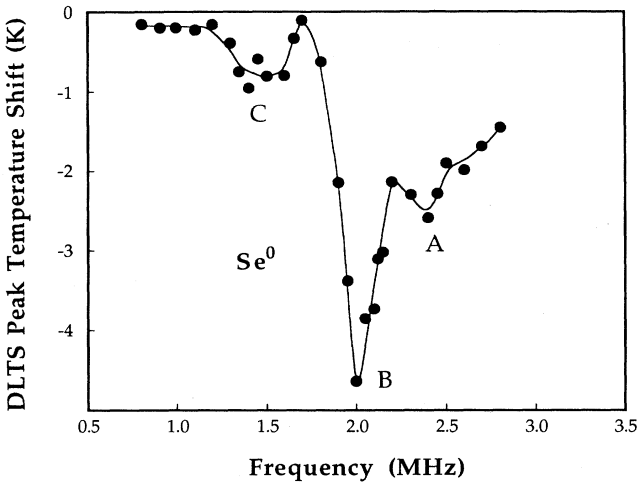

FIG. 5. DLTS peak temperature shift vs frequency of vibrations for the Se^0 center. The solid lines is an aid to guide the eye.

represent the ionized center and its bound state, respectively. For deep impurity centers with considerable lattice relaxation, the multiphonon excitation process may be followed either by a tunneling process through a potential barrier (process 1 in Fig. 6) or a transition over point B (process 2).[12] At low temperatures, when the emission rate is small, process 1 is more probable than process 2. Since a periodic displacement of a deep impurity center cannot explain an increased thermal ionization of the center in adiabatic approximation, two other possible explanations for the observed effect are to be considered. The first explanation implies thermoelastic losses of the mechanical energy. Heating due to the compression of the samples is expected to increase the emission rate. A possible second explanation should take into account nonlinear effects originating from oscillating stresses in solids. In particular, one would expect static strains which are associated with propagating acoustic waves when anharmonic terms in the crystal potential are taken into account. Changes in thermal emission rates due to pressure are well documented for deep levels in semiconductors.[13]

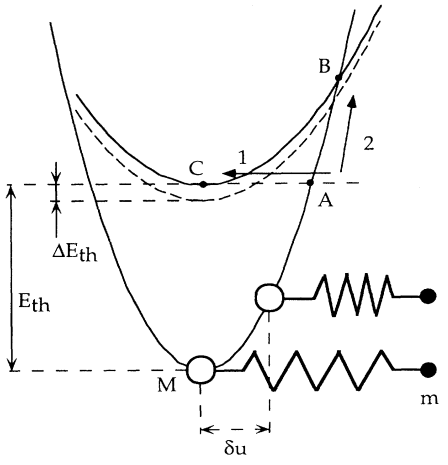

FIG. 6. Schematic energy diagram in the adiabatic approximation. The lower curve represents the initial state with an electron captured by the impurity atom. The upper curve corresponds to an empty center and an excited electron. δu is the shift in the equilibrium position of the impurity atom M due to low-frequency vibrations (see text for details). m if the mass of the silicon atom.

It has already been mentioned in Sec. II that special care was taken to ensure temperature uniformity in our samples. The thermal relaxation time in silicon is expected to be at least in the μs range, i.e., much shorter than the integration time of our spectrometer. However, it should be realized that the thermocouple in our setup measured the temperature at the surface, which is not a reliable measurement for measuring the internal sample temperature. This is particularly true when studying dynamical processes due to time-varying stresses in solids.

Nonetheless, compelling evidence that the observed enhancement of the emission rate cannot be explained by an increase in temperature was obtained from measurements when the perturbation of our samples was performed by ultrasonic tonebursts. Figure 7 presents DLTS peak shifts for the selenium centers plotted against the ultrasonic toneburst delay time t_d [see Fig. 2(b)]. It is easily seen that the enhancement of the emission rate for the Se^0 center is characterized by delay times in the ms range. It is also seen that corresponding shifts in the DLTS peak position for the charged center vary only very slowly with t_d. Unfortunately, technical reasons did not allow us to measure shifts at very small values of the delay time.

Although the DLTS method is not very accurate for such measurements, the data in Fig. 7 nevertheless sug-

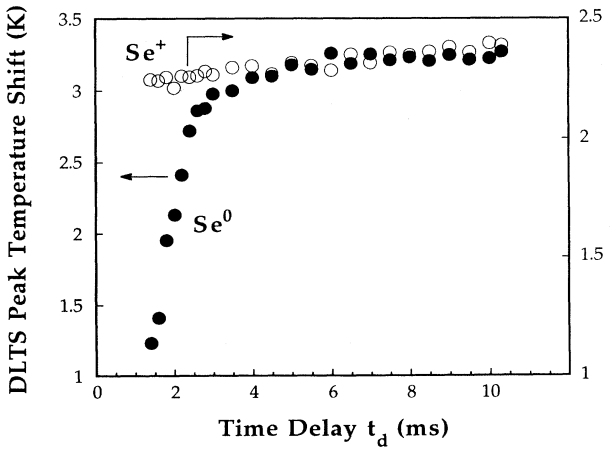

FIG. 7. Shift of the DLTS peak temperature vs time delay t_d for the selenium centers. Rate window, filling pulse width, and rf were 30 s^{-1}, 0.2 ms, and 2.00 MHz, respectively. $\tau_v = 20$ ms and $t_d = t_{d1} = t_{d2}$ [Fig. 2(b)].

gest that the observed effect is not consistent with heating. It is difficult to explain how the same center in different charge states can exhibit markedly different time dependencies if the observed shifts were due to heating effects.

Further measurements were performed using the toneburst configurations (c) and (d) of Fig. 2 in order to obtain further evidence. Curve 1 (open circles) in Fig. 8 was obtained by applying ultrasonic tonebursts simultaneously with the filling pulses [(a) and (d) in Fig. 2]. If instead an ultrasonic toneburst was inserted during the capacitance transient [(a) and (c) in Fig. 2], the vibrational excitation yielded considerably larger changes in the DLTS peak shift (curve 2; filled circles in Fig. 8). For $\tau_v=\tau_p$ [configuration (d)], the change in the DLTS peak position is still rather small even for large values of the duty cycle $(\tau_v/t_0)\approx 0.7$. At the same time, when $\tau_v=(t_0-\tau_p)$, the change is already large for $(\tau_v/t_0)\approx 0.3$. The data presented in Figs. 7 and 8 obviously show that the enhancement of the emission rate is not explained by an excitation of thermal phonons due to time-varying stresses.

Our results are better explained by nonlinear effects. Two factors come to mind: (i) externally applied vibrations may produce static strains in solids, and (ii) impurity atoms involved in the low-frequency oscillating motions may change their equilibrium position. The phenomenon of static strains was previously predicted for acoustic waves,[14] and experimentally observed in silicon.[15,16] The final energy state corresponding to an ionized center and a free electron can be reduced in the presence of static strains as shown in Fig. 6 by the dashed potential curve. The decrease in energy, $\Delta E_{\rm th}$, lowers the width and height of the potential barriers ABC and, hence, increases the electron emission probability. The change of the emission rate is readily calculated from the detailed balance relationship[17]

$$e_n^t=\sigma_n^t v_{\rm th} N_c \exp(-E_{\rm th}/kT)\ , \tag{2}$$

where σ_n^t is the capture cross section, $v_{\rm th}$ is the thermal velocity of electrons in the conduction band, and N_c is the effective density of states in the conduction band. As shown in Ref. 16, the strength of the static component depends on the amplitude of the applied strain squared. Considering $\Delta E_{\rm th}$ to be a linear function of stresses and taking into account Hooke's law, one would expect a square dependence of $\Delta E_{\rm th}$ on the amplitude of applied stresses. This in turn implies that the change of the logarithm of the emission rate is proportional to $A_{\rm in}^2$:

$$\Delta(\ln e_n^t)\sim\Delta E_{\rm th}\sim A_{\rm in}^2\ . \tag{3}$$

Figure 9(a) shows the logarithm of the emission rate versus the square of the applied voltage amplitude $A_{\rm in}$. Within the scatter of the experimental data, the curves for the different centers are indeed linear. No change in the linear dependence was observed for the Te centers when the temperature was decreased. Somewhat different

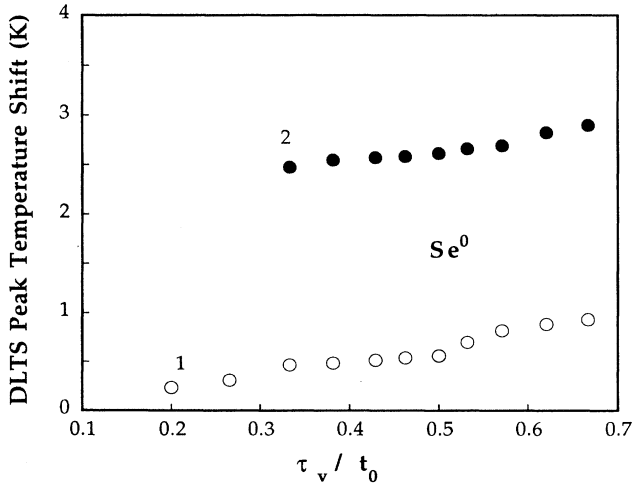

FIG. 8. DLTS peak temperature shifts vs duty cycle (τ_v/t_0) for the neutral selenium center. The open circles correspond to case (d) in Fig. 2; the filled circles represent configuration (c) in Fig. 2. The rate window was 121 s^{-1}, the filling pulse width ranged from 5 to 40 ms, and the rf was 2.00 MHz.

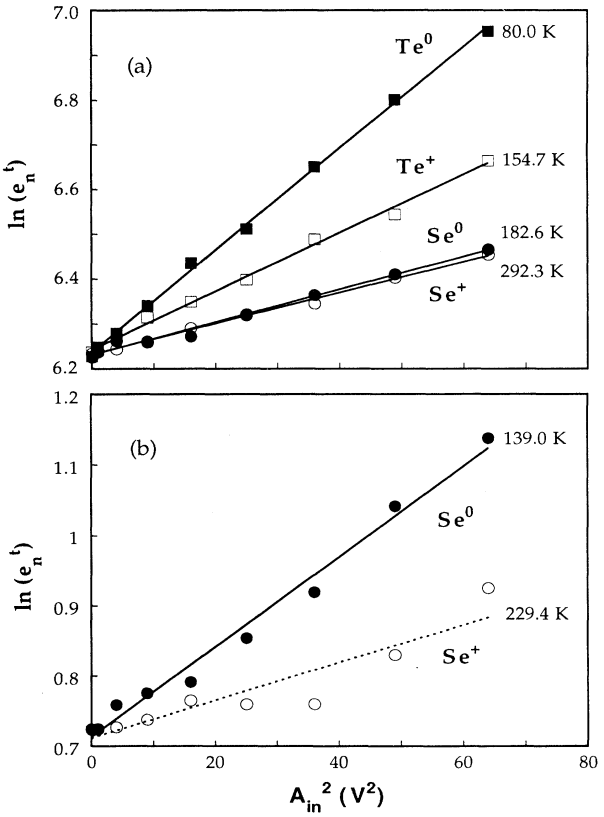

FIG. 9. Thermal emission rates vs $A_{\rm in}^2$ at different temperatures for all investigated centers. Lines are linear fits to the experimental data. The frequency of vibration was 2.00 MHz (Se-doped sample) and 1.92 MHz (Te-doped sample).

results were obtained for the selenium donors, which at least in the case of Se^+ show deviations from a linear dependence at lower temperatures [Fig. 9(b)].

As pointed out previously,[6] the activation energy E_{th} obtained from an Arrhenius plot of e_n^t is only equal to the change in enthalpy in the special case when the capture cross section σ_n^t is proportional to T^{-2}. Since the capture cross section was not measured in this study, and previous studies have shown that $\sigma_n^t \sim T^{-x}$ where x is close to 2,[1] we have plotted our data in Fig. 10 as $\log_{10} e_n^t$ versus $10^3/T$ for the charged and neutral selenium donors with (filled circles) and without (open circles) resonant vibrations. In all cases a linear dependence was observed. Changes in activation energy due to varying vibrational amplitudes A_{in} obtained from such Arrhenius plots are plotted in Figs. 11 and 12 for all centers investigated. The effect of resonant vibrations on the thermal activation energy was remarkably large for the charged and neutral tellurium centers. The decrease in E_{th} varies linearly with A_{in}^2 as expected from Eq. (3).

Rather different results were obtained for the selenium centers. Whereas the charged center was practically unaffected by resonant vibrations, a considerable decrease of the activation energy not described by Eq. (3) was observed for the neutral center. This is in agreement with the data exhibited in Fig. 9, which showed that the enhancement of the emission rate was smallest for the Se^+ center in comparison with other investigated centers.

Essentially identical results were obtained when the Se centers were perturbed by propagating acoustic waves. Corresponding changes of ΔE_{th} for the charged and neutral selenium donors are shown in Fig. 11. Also in this case the activation energy of the Se^+ center was almost

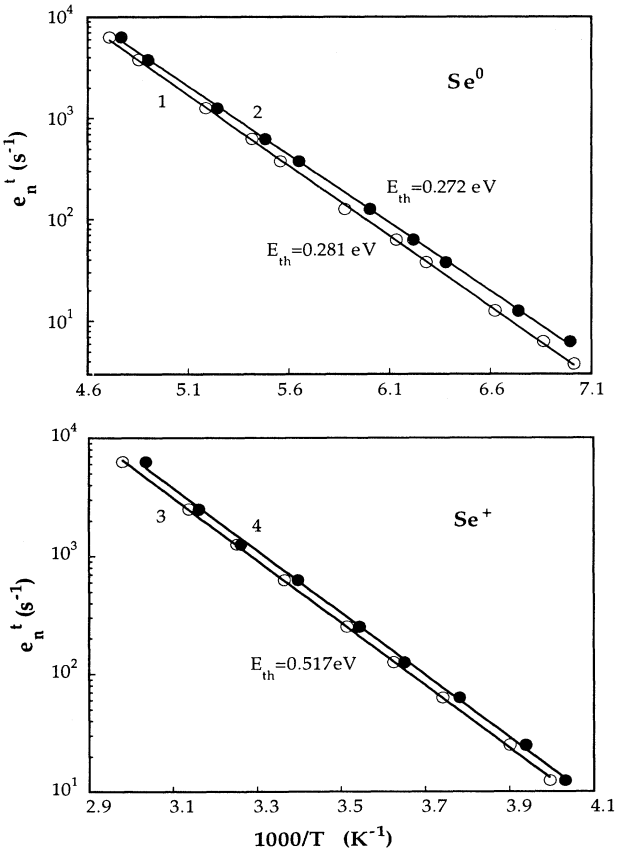

FIG. 10. Arrhenius plots of thermal emission rates of the Se^0 (1,2) and Se^+ (3,4) centers without vibrational excitation (1,3) and with $A_{in}=8$ V (2,4). The frequency of vibration was 2.00 MHz. Energies given are activation energies as discussed in the text.

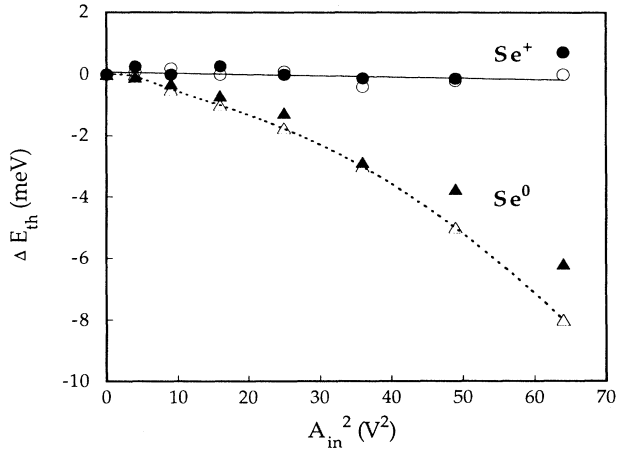

FIG. 11. Change in the thermal activation energy vs A_{in}^2 for the Se^+ and Se^0 centers. The open circles and triangles correspond to resonant vibrations at 2.00 MHz, the filled circles and triangles to Lamb waves at 1.64 MHz. The solid line is a linear fit to the open circles, while the dashed line is a smooth fit to the open triangles.

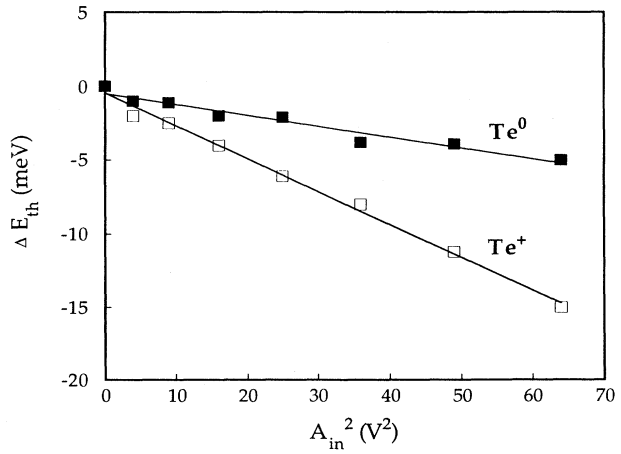

FIG. 12. Change in the thermal activation energy vs A_{in}^2 for the Te^+ and Te^0 centers due to resonant vibrations at 1.92 MHz. The lines are the linear fits to the experimental data.

unaffected by the external perturbation, whereas the data for the Se^0 center were very similar for both resonant vibrations and acoustic waves. However, one has to bear in mind that these data were obtained for different stress fields inside the samples which are not discussed in this paper.

IV. DISCUSSION

The results so far presented suggest that the enhancement of the thermal emission rate of electrons obviously originates from nonlinear effects in combination with oscillating mechanical stresses. If it is assumed that the observed effect originates from static strains, it is worth considering whether or not the results can be interpreted within the deformation-potential approximation.[18] Following the analysis performed in Ref. 7, one can then assume that the electron states of chalcogen donors in silicon under uniaxial stress are well described by the shift of the conduction-band minimum. Considering stresses along the $\langle 001 \rangle$ direction, the decrease in energy $\Delta E_{\rm th}$ exhibited in Fig. 6 is then given by

$$\Delta E_{\rm th} = 2\Xi_u (s_{11} - s_{12})\theta/3 \tag{4}$$

for compression, and by

$$\Delta E_{\rm th} = \Xi_u (s_{11} - s_{12})\theta/3 \tag{5}$$

for dilatation. Here Ξ_u is the shear deformation potential, s_{11} and s_{12} are components of the elastic compliance tensor, and θ is the absolute value of the applied stress. To simplify our evaluation, it is assumed that the nonlinear analysis of a lossless semi-infinite solid performed in Ref. 16 can be applied to our problem of waves in a thin plate and resonant sample vibrations. It is further anticipated that only atomic displacements u parallel to the chosen $\langle 001 \rangle$ direction occur. This implies that only pure longitudinal waves are considered. With these assumptions, the static strain can be expressed as

$$(\partial u/\partial z)_{\rm stat} = (\beta/8)(2\pi f u_0/v)^2 , \tag{6}$$

where β is an acoustic nonlinearity parameter, and f and v are the frequency and sound velocity, respectively. u_0 is the amplitude of the atomic displacement, which can readily be expressed as a function of the amplitude of the applied stress θ_0:

$$u_0 = (v/2\pi f c_{11})\theta_0 , \tag{7}$$

where c_{11} is a component of the elastic stiffness tensor. Taking $\theta_0 \sim 5\times 10^5$ N/m^2 (see Sec. II), $f = 2\times 10^6$ s^{-1}, $v = 8.43\times 10^3$ m/s,[19] and $c_{11} = 16.56\times 10^{10}$ N/m^2,[20] the static strain $(\partial u/\partial z)_{\rm stat}$ will be of the order of 2×10^{-12} if $\beta = 2$ is assumed.[15] This gives an estimated value for the static stress $\theta_{\rm stat}$ of about 0.4 N/m^2, which is about six orders of magnitude smaller than θ_0. Taking into account the experimentally observed dilatation of the silicon samples in the presence of acoustic waves,[16] Eq. (5) gives $\Delta E_{\rm th} \sim 1\times 10^{-11}$ eV for $\Xi_u = 8.5$ eV,[7] and $s_{11} - s_{12} = 9.745\times 10^{-12}$ m^2/N (Ref. 20) in the case of Se^0. Moreover, substituting the value for θ_0 into Eq. (4) yields a value of 1.4×10^{-5} eV for $\Delta E_{\rm th}$. All calculated $\Delta E_{\rm th}$ values are much smaller than the experimentally observed values.

The analysis performed clearly shows that the deformation-potential approximation obviously is not the correct model for describing the physical processes originating from externally applied oscillating stresses. To the best of our knowledge, theoretical considerations regarding the effect of ultrasonic vibrations on the thermal emission of electrons from deep centers in semiconductors have not yet been performed. For shallow centers it has been suggested that the enhancement of thermal emission rates is expected to originate either from quasistatic tunneling or multiphonon absorption. However, theoretical considerations showed that these processes may only be observed in piezoelectric crystals.[21] An attempt is therefore made to present a qualitative model which tentatively explains the obtained data in a different framework.

The model is based on the assumption that impurity atoms which take part in low-frequency oscillating motions exhibit high-frequency harmonic vibrations around a different equilibrium position. Although our experimental data did not definitively resolve this issue, they did provide strong evidence of such an approach. First of all, nonlinear displacements δu of impurity atoms are required to give the linear dependencies shown in Figs. 9 and 12. Assuming that the lattice and impurity atoms are described by a single configuration coordinate model, the change $\Delta E_{\rm th}$ of the bottom of a potential well $V(r)$ for a bound electron is then a linear function of δu:

$$\Delta E_{\rm th} \sim V(r)\delta u . \tag{8}$$

As in the case of static strains which have been analyzed above, the nonlinear displacement δu arises from higher-order terms of the lattice-defect interatomic potential. Hence we would expect $\Delta E_{\rm th}$ to be proportional to the square of the applied voltage $A_{\rm in}$ as plotted in Fig. 12.

It may also be relevant to note that beyond the qualitative similarity of the two branches of the crystal anharmonicity which resulted in the appearance of the static strains and displacements δu, there is an important quantitative difference. When analyzing static strains, it becomes obvious that the energy shifts of Eqs. (3)–(5) originate generically from impurities which have been subjected to static strains within the deformation-potential approximation. On the other hand, the nonlinear displacement of impurity atoms with respect to their surroundings would result in changes of the activation energy in accordance with Eq. (8). However, the deformation-potential approximation leads, as discussed above, to erroneously small values of $\Delta E_{\rm th}$.

As far as we are aware, experimental data about the strength of the electron-lattice coupling are not available for any of the chalcogen-related donors. Nevertheless, recent theoretical studies of the lattice relaxation of deep levels in silicon allow us to perform a simple numerical evaluation of our model. According to Ref. 22, it is reasonable to assume that the binding energy of chalcogen-related donor levels varies about a hundred meV due to a relaxation of neighboring atoms of up to

5%. Taking a value of about 10 meV for ΔE_{th}, as deduced from Figs. 11 and 12, one obtains a value of about 0.5% for the lattice relaxation. This estimate yields $\delta u \approx 2.7 \times 10^{-2}$ Å. It is not unreasonable to assume that such nonlinear shifts are feasible, considering that the amplitude of vibrations was roughly 0.2 Å [see Eq. (7)].

Our model also seems to be consistent with the observed delay of the Se^0 center shown in Fig. 7. It is assumed that in order to obtain a shift δu, the center needs a certain number of vibrational periods, and that the delay times therefore are characterized by the damping properties of the defect. This effect, however, remains to be confirmed by further investigations, since, as mentioned in the Sec. III, the DLTS technique is not very suitable for time-resolved measurements.

It is also believed that a large increase in the activation energy should be observed for defects with strong relaxation and nonsymmetric configurations. We could not find such large effects for the selenium and tellurium donors in silicon, in agreement with previous suggestions that these centers are not expected to exhibit strong lattice relaxations.

Expanding the potential energy Φ of two interacting atoms in a Taylor series, one obtains

$$\Phi(r)=\phi(r_0)+(\partial\phi(r)/\partial r)_0 u+\tfrac{1}{2}(\partial^2\phi(r)/\partial r^2)_0 u^2 + \tfrac{1}{6}(\partial^3\phi(r)/\partial r^3)_0 u^3+\cdots , \quad (9)$$

where $\phi(r)$ is the potential energy function of the two atoms separated by a distance r. $u=r-r_0$ is the displacement from the undeformed value r_0, and the third-order term describes the nonlinear lattice behavior and, in particular, the thermal expansion of the crystal. Using Eq. (9), it can be shown that the change δu in the separation of the two atoms is given by the ratio of the second and third derivatives of the energy function ϕ. For the sake of simplicity, we assume that this function is Born-Mayer-like,[23,24] and given by

$$\phi(r)=A\exp[-\rho(r-r_0)/r_0] , \quad (10)$$

with two parameters A and ρ, such that we can write

$$\delta u \sim r_0/\rho . \quad (11)$$

It may therefore be concluded that in our case changes in emission rates are governed not by the strength of the defect-lattice potential [the preexponential factor A in Eq. (10)], but by the "hardness" parameter ρ and a nondeformed atomic pair separation r_0. This could be the main difference and advantage of the perturbation technique described in this paper in comparison with the commonly used uniaxial-stress experiments. It should therefore be possible to obtain additional information about the type of interaction in the defect-lattice system (parameter ρ) and local impurity configuration [r_0 in Eq. (11)] from this kind of measurement.

The observed changes in the activation energies of the neutral Se and Te donors are very similar, as shown in Figs. 11 and 12. This could have been anticipated by taking into account previous results obtained for chalcogen-related centers in silicon.[1] However, the difference in the Se^+ and Te^+ behavior (Figs. 11 and 12) is not predicted by these studies, and is one of the most striking results of the present study. It is too early to speculate about why the response of the Se^+ center on the external vibrational perturbation is so small in comparison with the other investigated donors, since our evaluation has been too simple in order to be useful for a quantitative analysis. Whether this is due to differences in the interaction of the Se^+ ions with neighboring atoms [Eq. (11)], or originates from an increase of the multiphonon excitation process (Fig. 6), remains to be shown.

V. CONCLUSION

We have observed an enhancement of the electron emission from selenium and tellurium double donors in silicon due to externally applied mechanical vibrations in the MHz frequency range. The enhancement is tentatively attributed to a displacement of the equilibrium position of impurity atoms subjected to an oscillating stress. Our data suggest that the shifts depend upon the "hardness' parameter of the interatomic potential and the local impurity configuration rather than on the strength of the impurity-lattice interaction. The method of external perturbation used in this study seems to offer interesting possibilities for the characterization of defects with nonsymmetric configurations and large lattice relaxation. A better theoretical understanding of the observed effects and of defect perturbations by ultrasonic vibrations in general is needed in order to improve further studies.

ACKNOWLEDGMENT

One of us (O.A.K.) thanks the Swedish Institute for financial support of this work.

*Permanent address: Faculty of Physics, Kiev University, Kiev 252022, Ukraine.

[1]See the review by H. G. Grimmeiss and E. Janzen, in *Handbook of Semiconductors,* edited by T. S. Moss (North-Holland, Amsterdam, 1994), Vol. 3B, pp. 1755–1888.

[2]I. V. Ostrovskii, Pis'ma Zh. Eksp. Teor. Fiz. **34**, 467 (1981) [JETP Lett. **34**, 446 (1981)]; I. V. Ostrovskii and O. A. Korotchenkov, Solid State Commun. **82**, 267 (1992).

[3]S. S. Ostapenko, L. Jastrzebski, J. Lagowski, and B. Sopori, Appl. Phys. Lett. **65**, 1555 (1994); I. A. Buyanova, A. U. Savchuk, M. K. Sheinkman, and M. Kittler, Semicond. Sci. Technol. **9**, 2042 (1994).

[4]A. S. Nowick and B. S. Berry, *Anelastic Relaxation in Crystalline Solids* (Academic, New York, 1972).

[5]M. Kleverman, H. G. Grimmeiss, A. Litwin, and E. Janzen, Phys. Rev. B **31**, 3659 (1985).

[6]H. Pettersson and H. G. Grimmeiss, Phys. Rev. B **42**, 1381 (1990).

[7]K. Bergman, G. Grossmann, H. G. Grimmeiss, M. Stavola, and R. E. McMurray, Jr., Phys. Rev. B **39**, 1104 (1989).
[8]I. A. Viktorov, *Rayleigh and Lamb Waves* (Plenum, New York, 1967).
[9]D. V. Lang, J. Appl. Phys. **45**, 3023 (1974).
[10]H. G. Grimmeiss, E. Janzen, and B. Skarstam, J. Appl. Phys. **51**, 3740 (1980).
[11]H. G. Grimmeiss, E. Janzen, H. Ennen, O. Schirmer, J. Schneider, R. Wörner, C. Holm, E. Sirtl, and P. Wagner, Phys. Rev. B **24**, 4571 (1981).
[12]*Solid State Physics,* edited by R. Kubo and T. Nagamiya (McGraw-Hill, New York, 1969).
[13]G. A. Samara, Phys. Rev. B **39**, 12 764 (1989); M. F. Li, P. Y. Yu, E. Bauser, W. L. Hansen, and E. E. Haller, Semicond. Sci. Technol. **6**, 825 (1991).
[14]R. N. Thurston and M. J. Shapiro, J. Acoust. Soc. Am. **41**, 1112 (1967).
[15]J. Philip and M. A. Breazeale, J. Appl. Phys. **52**, 3383 (1981).
[16]W. T. Yost and J. H. Cantrell, Jr., Phys. Rev. B **30**, 3221 (1984).
[17]O. Engström and A. Alm, Solid-State Electron. **21**, 1571 (1978).
[18]C. Herring and E. Vogt, Phys. Rev. **101**, 944 (1956).
[19]E. Dieulesaint and D. Royer, *Elastic Waves in Solids* (Wiley, Chichester, 1980).
[20]J. J. Hall, Phys. Rev. **161**, 756 (1967).
[21]V. V. Popov and A. V. Chaplik, Fiz. Tekh. Polopruvodn. **10**, 1780 (1976) [Sov. Phys. Semicond. **10**, 1061 (1976)].
[22]J. E. Lowther, J. Phys. C **13**, 3665 (1980).
[23]P. B. Ghate, Phys. Rev. **139**, A1666 (1965).
[24]Y. Hiki and A. V. Granato, Phys. Rev. **144**, 411 (1966).